EUROPEAN ORGANIZATION FOR NUCLEAR RESEARCH

CERN - PS DIVISION

CERN/PS 93-34 (LP)
CLIC Note 209

PULSE TRAIN GENERATION AT 209 NM

P.M. Devlin-Hill

Abstract

A pulse train generator designed to operate at 209 nm was required for the CLIC test facility (CTF). The function of the generator is to provide, from a single laser pulse produced by the main Nd:Ylf laser system, a train of laser pulses. A train of eight laser pulses of equal intensity and separated by a time interval of one 3 GHz period is required in the CTF to produce 30 GHz power for RF structure tests.

In this paper some of the types of beam splitting optics which may be used at 209 nm and the generator systems which can be built from them are introduced. A method of setting the timing between the pulses to sub-picosecond accuracy is presented. A number of factors which can limit system performance are discussed. Some computational and experimental results are presented.

Workshop on High Intensity Electron Sources, Legnaro Padova, Italy, 24 - 28 May 1993

Geneva, Switzerland
26/7/93

Pulse train generation at 209 nm

P.M.Devlin-Hill

CERN, CH-1211 Geneva 23

Abstract

A pulse train generator designed to operate at 209 nm was required for the CLIC test facility (CTF). The function of the generator is to provide, from a single laser pulse produced by the main Nd:Ylf laser system, a train of laser pulses. A train of eight laser pulses of equal intensity and separated by a time interval of one 3 GHz period is required in the CTF to produce 30 GHz power for RF structure tests.

In this paper some of the types of beam splitting optics which may be used at 209 nm and the generator systems which can be built from them are introduced. A method of setting the timing between the pulses to sub-picosecond accuracy is presented. A number of factors which can limit system performance are discussed. Some computational and experimental results are presented.

1 Introduction

The CLIC (CERN Linear Collider) Test Facility or CTF was set up to start work on the development of new methods and technologies required to construct a linear collider with a 2 TeV centre-of-mass energy. To achieve the required accelerating gradient of 80 MV/m it was proposed to use an RF gun equipped with a laser-driven photocathode to provide high intensity electron bunches, and to accelerate these to 60 MeV or more using a 3 GHz TW structure before allowing them to pass through CLIC Accelerating Structures (CAS). Calculations [1] show that the RF power generated per CAS filling time by a single electron bunch is virtually the same as that generated by a train of electron bunches of the same total charge as the single bunch. The advantage of using a train of bunches is that the task of the gun is alleviated and the effects of space charge reduced. It was proposed to produce this train of electron bunches by firing a train of laser pulses at the photocathode of the gun. In a simplified scheme for 30 GHz power generation in the CTF [2] a train of eight pulses of approximately equal intensity and separated by a time interval of one 3 GHz period, i.e. 333 ps, is required. Extension to a sixteen pulse train is envisaged.

In this paper a study of a particular type of pulse train generator (PTG), which could be used to generate the required train of laser pulses, is presented. A list of abbreviations used is appended.

2 General system design

For reasons to be discussed in sections 3 and 4 the most appropriate system design would appear to be that illustrated schematically in figure 1(a). The geometrical configuration of this system is not new, such a system having been used [3] to generate two trains of 16 pulses (of pulse width 60 ps) with a pulse separation of 350 ps at 532 nm. In the present paper the different types of optics which may be used to build these systems, with particular emphasis on 209 nm, are introduced. A first attempt to develope an alignment technique accurate to the subpicosecond range is presented.

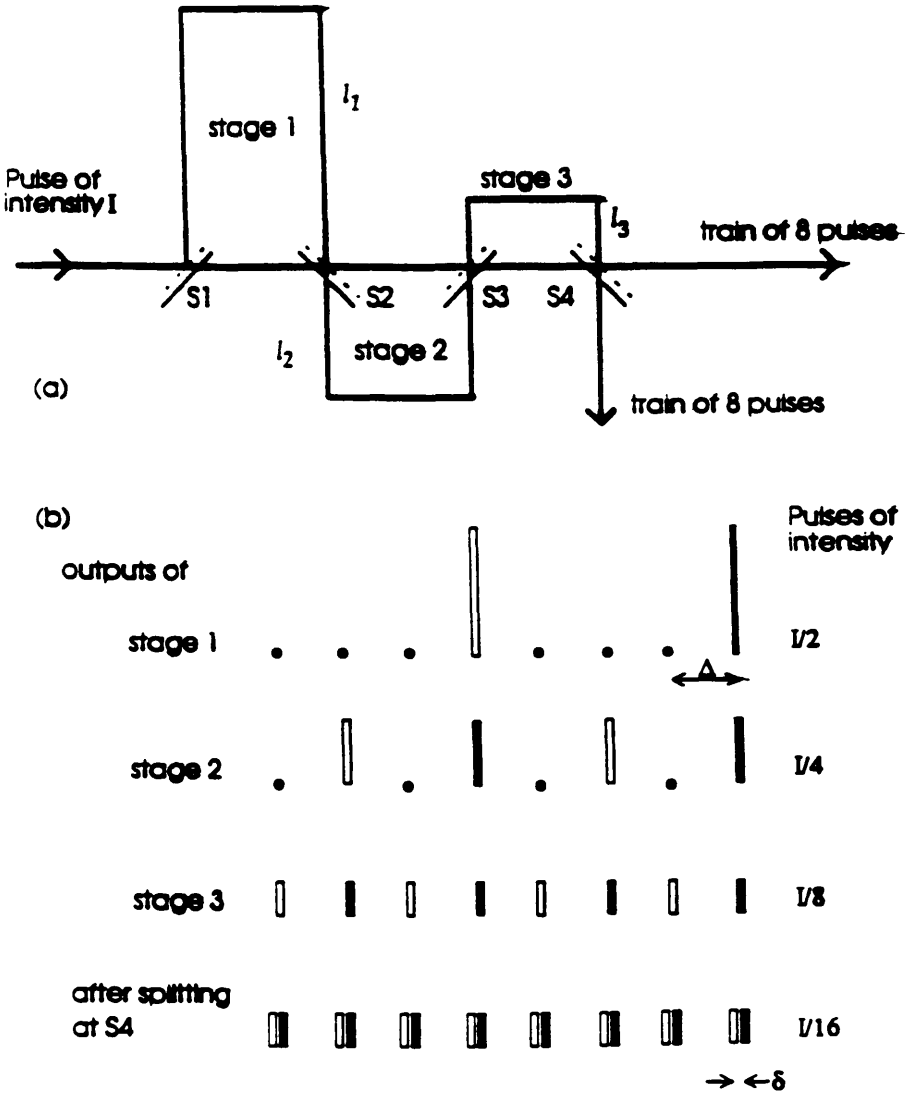

Figure 1: (a) Schematic of PTG geometry. S1 to S4 are beam splitters, the dashed line indicating the side of the substrate on which the beam splitter coating has been deposited. High reflectivity mirrors are not shown. l_1, l_2 and l_3 are the detour lengths of stages 1, 2 and 3 respectively. (b) Illustration of how the pulses within the train are generated. Black bars indicate pulses taking a straight through path in a stage and white bars those that take a detour (cf text).

In the ideal case the system would be such that a single pulse of intensity I from the synchro-laser system (a Nd:Ylf system [4]) would, on entering the PTG as shown in figure 1(a), be consecutively split into transmitted and reflected pulses of equal magnitude on each encounter with a beam splitting optic. Using four beam splitters marked S1 to S4, two trains of eight pulses travelling in mutually orthogonal directions would be generated at the output. The timing between the pulses within the train would be determined by the detour lengths, l_1, l_2 and l_3, of the various stages. By appropriately setting l_1 the two pulses output by stage 1, would be separated in time by an interval of $4x\Delta$, where nominally $\Delta = 333$ ps, and would each have an intensity of I/2 as shown in figure 1(b). The pulses generated by the beam splitter S1 are said to have reached the output of stage 1 when they are coincident with the beam splitter coating of S2, indicated by a dashed line, but before they have interacted with it. The outputs of stages 2 and 3 are similarly defined. By correctly setting l_2 and l_3 the pulses output by stage 2 would be separated in time by an interval of $2x\Delta$ and have an intensity of I/4 and those pulses output by stage 3 a pulse separation of Δ and an intensity of I/8. At S4 the intensity of the pulses would be reduced to I/16 and a delay δ, determined by the substrate thickness of S4, would be introduced between the two trains of eight.

The system geometry is such that it facilitates

1. the rapid and accurate alignment of the mirrors and beam splitters within the system
2. the use of interferometry to set the timing between the pulses of the train

In other systems [5] the RF structures under test are used to set the timing between the pulses. In such systems the distances between the optics are adjusted by observing transmission through the RF structures. However using the systems described in this paper the timing between the pulses in the train may be set independently of the RF structures. An independent reference is therefore provided.

The study of space charge or wakefield effects between the different pulses of the train is facilitated by the fact that pulses may be individually selected. Unlimited free choice of various pulse combinations for such studies is not possible, for example it is not possible to simultaneously select the first and eighth pulses of the train but a good selection of pulse combinations is available.

Provided that the optics used have a small wedge angle, all the pulses within the train will travel in a single direction along a single beam line, of length 20m, to the photocathode. As a consequence;-

1. any alignment or timing errors between the different pulses of the train will be restricted to those of the PTG system itself
2. all the pulses arriving at the photocathode will arrive with their wavefronts tilted to the same degree
3. any additional optics such as telescopes or image relays for example may be easily inserted into the beam line.

One disadvantage of the system is that as two trains are produced but only one used for RF structure tests not all of the available laser energy is employed in the production of the electron bunches. The second train may however be used for diagnostic purposes.

3 Intensity balancing

3.1 Choice of optics

3.1.1 Beam splitters

Timing considerations aside, the most versatile means of beam splitting is to use polarizing beam splitters designed to operate at the Brewster angle. However the Brewster angle does not facilitate an accurate or convenient method of setting the timing between the pulses of the train. In any case at 209 nm this option is not open because of the unavailability of two materials of sufficiently different refractive index and low absorption required to make such an optic. Similarily polarizing beam splitters designed to operate at 45° are not available.

There are however other types of intensity splitters which may be used at an angle of incidence (AOI) of 45° these being;-

1. nonpolarizing intensity splitters
2. S-polarization intensity splitters
3. P-polarization intensity splitters
4. Unpolarized intensity splitters

An example of a best case nonpolarizing intensity splitter for 262 nm is presented in figure 2. Ideally the P and S polarization curves would touch at the design wavelength rendering the splitting ratio of the optic completely independent of the state of polarization of the incident light. The splitting ratio is therefore fixed and an intrinsic property of the optic itself. From figure 2, even at 262 nm, in the optimum case, the P and S curves can not be made to touch. The separation of the curves can be expected to be larger at 209 nm.

Typical transmission curves for S-polarization intensity splitters,

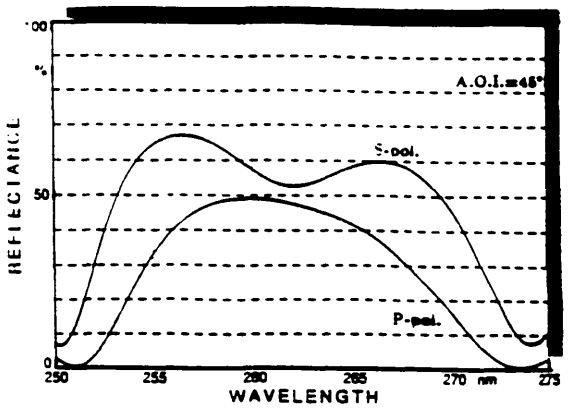

Figure 2: Nonpolarizing intensity splitter designed for 262 nm. Note that P- and S-polarization curves do not quite touch at the design wavelength. Supplied by [6].

P-polarization intensity splitters and unpolarized intensity splitters are presented in figures 3, 4 and 5 respectively. In each case the transmission curves for the S and P polarization states are now separated from each other rendering the splitting ratio dependent on the state of polarization of the incident laser beam. On placing the S-polarization splitter, shown in figure 3, into an S polarized beam a 55:45 split should be obtained. However any depolarization of the incident laser beam away from its required S-polarized state will disturb the splitting ratio obtained at the optic. To minimize the influence of any depolarizing effects on the splitting ratio the P transmission curve should be placed as close as possible to the S transmission curve so that the characteristic of the optic approaches that of a nonpolarizing intensity splitter. A P-polarization intensity splitter is similiar to an S type but is used in a P-polarized beam. However, at 209 nm, these optics require twice as many layers in the multilayer thin film stack as a S-polarization splitter and will absorb more of the incident laser light [6]. The use of P-polarized intensity splitters is not to be recommended in systems where high reflectivity mirrors are

to be used since a high reflectivity mirror will reflect S-polarized light better than P-polarized light.

In an 'unpolarized' laser beam the splitting ratio obtained using an unpolarized intensity splitter will be the average of the individual S and P splitting ratios. If such a splitter were to be placed in a linearly polarized laser beam the splitting ratio obtained would be found to be a function of the azimuthal angle of the electric field vector of the incident light and to lie between the S splitting ratio and the P splitting ratio. In an experimental setup the splitting ratio obtained at this optic can be varied between these two values by placing a $\lambda/2$ waveplate in front of the optic. This property of the unpolarized intensity splitter may be optimized by making the curve separation as large as possible and by centring the curves on the nominally desired ratio.

3.1.2 Reflectors

Reflectors are required to provide the 180° detours around each stage. There are two types ;-

1. mirrors
2. total internal reflection prisms

In all of the systems to be described in this paper mirrors are used to provide the 180° detours. High reflectivity mirrors are available at 209nm and using the alignment techniques to be described it is possible to align pairs of mirrors to provide the 180° detours. Furthermore the use of mirrors facilitates the procedure required to set the timing between the pulses of the train.

Total internal reflection prisms are often used in systems when an accurate beam detour of 90° or 180° is required. However as described in reference [7] a

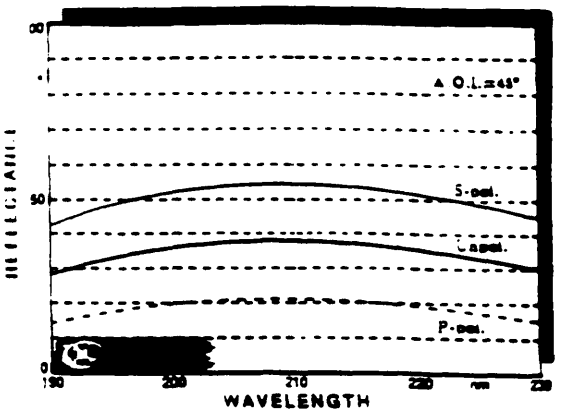

Figure 3: S-polarisation intensity splitter designed for 209 nm. Splitting ratio between the reflected and transmitted beams is 55:45. Supplied by [6].

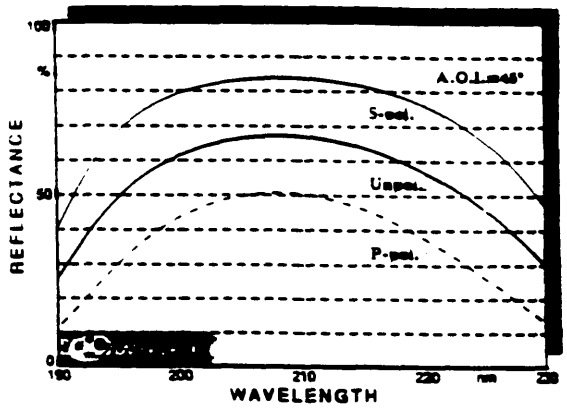

Figure 4: P-polarisation intensity splitter designed for 209 nm. Supplied by [6].

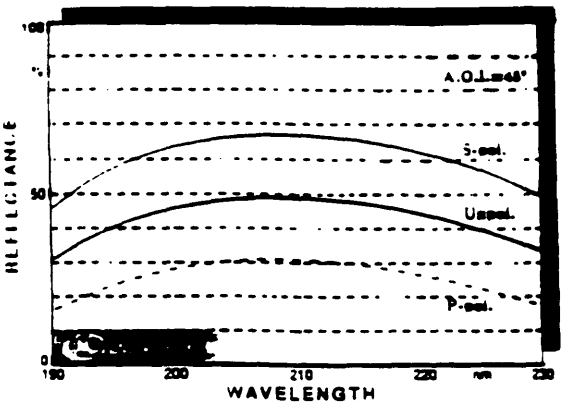

Figure 5: Unpolarized intensity splitter designed for 209 nm. Supplied by [6].

plane polarized wave will on total internal reflection become elliptically polarized. Therefore, timing considerations aside, the use of total internal reflection prisms in PTG systems should be considered carefully since the polarization content of the detoured beam may be disturbed.

3.2 Types of systems which may be built

There are two types of PTG systems which may be built using the types of optics described. These are ;-

1. simple systems
2. adjustable or compensated systems.

A simple system is one in which there is no control over the individual splitting ratios of the beam splitters. No provision is therefore made for the fact that the transmitted and reflected pulses, produced by any pulse incident on any splitter, will

1. suffer different losses
2. may experience different depolarizing influences

as they travel their different routes through the stage into which they have been injected. As a result the two pulses arriving for example at the beam splitter coating of the second splitter, S2 cf figure 1, will no longer be of equal intensity even if an exact 50:50 split had been obtained at the first splitter. The accumulative effect of uneven pulses each being equally split at each successive beam splitter and then being propagated through different routes will result in the observation of an uneven train at the output of the PTG system.

Pulses may also suffer different depolarizing influences as they travel through a stage. A depolarizing influence is any mechanism which rotates or phase shifts the pulse away from its required state of polarization. Since with the exception of the ideal nonpolarizing splitter, the splitting ratio of the optics discussed depends on the polarization of the incident pulse, any depolarization will disturb the splitting ratio experienced away from that required. Even in the absence of losses therefore an uneven train of pulses would be observed at the output of the generater.

In an adjustable or compensated system there is some control over the individual splitting ratios of the splitters and as a consequence the effects of different loss routes and depolarizing influences may be compensated for. Such a system, illustrated in figure 6, could be built using optimized unpolarized intensity splitters the splitting ratio at each being controlled through the use of a $\lambda/2$ waveplate. Waveplate W1 for example could be set to divert more light into the high loss route around stage 1 so that pulses T and R are equal on arrival at beamsplitter S2. Waveplate W2 could be similiarly adjusted so that the derivative of pulses R, i.e. RR and RT, will be equal on arrival at S3. Waveplate W3 can also be adjusted to ensure that pulses TT and TR, derived from T, are equal on arrival at S3. Problems however begin to arise at W4. Although it is possible to individually rotate TT and RR so that balanced pulses are produced at the exit of the next stage each, being composed of different mixtures of polarization states, requires a different waveplate setting. There is however only one waveplate to do the job. Waveplates W4 and W5 must therefore be set at an average setting and consequently at this point in the system an unavoidable modulation of the relative pulse intensity is introduced. Similiar problems will arise at waveplates

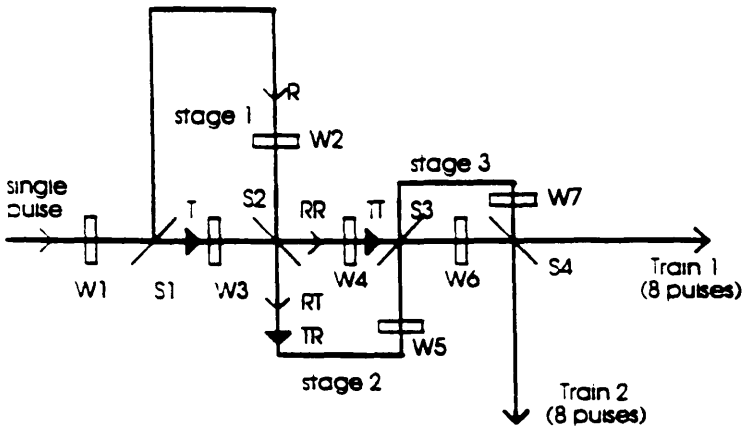

Figure 6: Adjustable or compensated PTG constructed from optimized unpolarized intensity splitters marked S1 to S4. W1 to W7 are $\lambda/2$ waveplates. High reflectivity mirrors are not shown. Pulse T produced by beam splitting at S1 generates pulses TT and TR at S2. Pulse R generates RR and RT.

W6 and W7 each of which will have four pulses to rotate for splitting at S4. Preliminary trials at 213 nm confirmed this problem.

3.3 Performance estimates for simple systems:Choice of system

Performance estimates for simple systems only will be presented here. Systems which may be built using nonpolarizing intensity splitters or P-polarization splitters are not considered since their use is not to be recommended. Three different types of system will be discussed ;-

- **System A**: built using S-polarization splitters only.

  In this system all the splitters are designed to give a 50:50 split for S-polarized light.

- **System B**: built using optimized unpolarized intensity splitters but which is a simplified version of the more sophisticated adjustable system.

  In this system the optimized unpolarized intensity splitters are such that their S and P polarization curves are centred on 50%. Therefore if the electric field vector of the input S-polarized light pulse is rotated through an angle of 45° by a $\lambda/2$ plate placed at position 3, cf figure 7, a 50:50 splitting ratio should be obtained at each splitter in the system.

- **System C**: built using three S-polarization splitters and a single optimized unpolarized splitter as the output splitter as specified for systems A and B.

  The intention of using an unpolarized splitter as S4, cf figure 7, was to prevent the laser energy from being divided equally into the two trains but to favour instead one train by diverting more energy into it. Train 1 for example can be favoured by placing a $\lambda/2$ waveplate in position 1 such that all the pulses which take the straight through path through stage 3, and which are nominally S-polarized, are rotated so

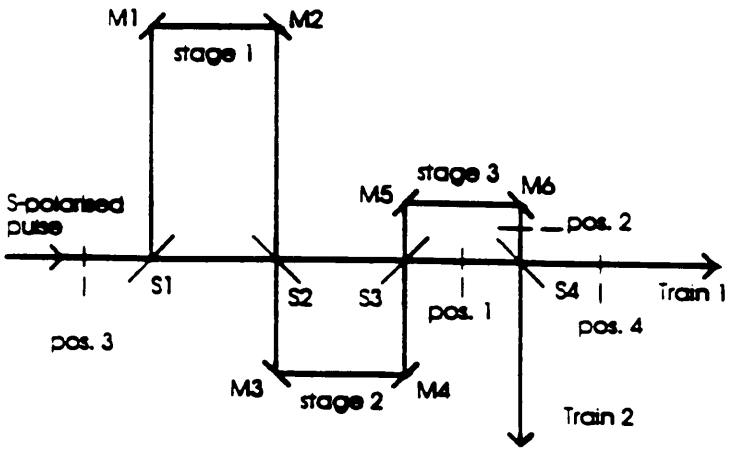

Figure 7: General layout of systems A, B, and C indicating positions (pos.1 to pos.4) where waveplates would be inserted. S1 to S4 are beam splitters and M1 to M6 are high reflectivity mirrors.

that they are P-polarized when incident on S4. In this case these pulses see a reflection:transmission ratio of 32:68. Therefore 68% of the pulse energy is directed into train 1. S-polarized pulses taking the detour around stage 3 are not rotated and on interaction with S4 will see a reflection:transmission ratio of 68:32. Therefore for these detoured pulses 68% of their energy is directed into train 1. Train 1 will now be composed of eight pulses, four of which are P-polarized and four S-polarized. To avoid additional modulation of these pulses as they are transported down the beam line to the photocathode a $\lambda/4$ waveplate should be placed at position 4. As a consequence all the pulses will become circularly polarized and will see average P and S polarization losses at each mirror encountered. Train 2 can be similiarly favoured by placing a $\lambda/2$ plate in position 2 only.

For each system the expected performances were calculated taking into account the losses that each pulse will see as a function of its polarization state at each antireflection, mirror and splitter coating it encounters. The information [6] used to carry out these calculations is presented in table(1) in which estimated

	Typical Performance Characteristics at 209nm							
	no absorption+scatter				with absorption+scatter			
	% Reflection		% Transmission		% Reflection		% Transmission	
	P	S	P	S	P	S	P	S
M	97	99.5	-	-	94	96.5	-	-
UNP	32±2(7)	68 ±2(7)	68 ±2(7)	32 ±2(7)	31±2(7)	67 ±2(7)	67 ±2(7)	31 ±2(7)
S	50 ±2(7)	50 ±2(7)	50 ±2(7)	50 ±2(7)	49 ±2(7)	49 ±2(7)	49 ±2(7)	49 ±2(7)
AR	-	-	99.9	99.2	-	-	98.9	98.2

Table 1:Typical performance characteristics of a high reflectivity mirror (M), unpolarized intensity splitter (UNP), S-polarization intensity splitter (S) and an antireflection coating (AR) at 209 nm. P and S stand for P polarization and S polarization respectively. Data supplied by [6].

performance characteristics are given for the case in which absorption and scattering occurs in the dielectric coating (real case) and for that in which it is assumed not to (design case). In the calculations absorption and scattering have been taken into account. Data relating to the beam splitters has been given with error bars. An error of ±2% may arise due to inaccuracies in monitoring during film deposition. An additional shift of ±5% may occur due to ambient environment and exposure to the laser radiation itself.

As the characteristics of each optic, due to the factors mentioned above, are likely to differ from those specified the performances of systems A,B,C, cf tables (2),(3),(4), respectively, were calculated at a number of values corresponding to expected shifts in coating performance;- marked departure from specification on the tables presented. In these calculations any depolarization effects have been neglected i.e. pulses are always assumed to be linearly polarized.

Defining a good system as one which provides the highest beam transmission and best %PHM (ratio of smallest pulse intensity to largest pulse intensity) for each specification, and the expected departures from that specification, System C would appear to be the best choice. It was this system which was constructed and RF structure tests were carried out using Train 1.

3.4 Factors limiting system performance with respect to intensity balancing

The factors which will limit system performance are listed below ;-

1. depolarization of input beam
2. tolerance of and shifts in beam splitter coating specification
3. alignment errors
4. dirty/dusty environment
5. coating damage due to (4) above or due to insufficient beam expansion
6. substrate losses
7. birefringence in substrate
8. wavefront distortion

All of the systems described depend for their correct operation on the polarization of the input beam being correctly defined. For example although the 209 nm pulse provided by the synchro-laser system is produced by harmonic generation this is not an adequate assurance that the pulses arriving at the input of the PTG will be well polarized. Depolarization may occur, due to strain birefringence, in the windows of the cells in which the harmonic generators are mounted and at any optic such as telescopes and mirrors placed in the beam path.

As has been discussed in section 3.3 an uncertainity of ±2% may occur in the specification of the beam splitter coatings and a further shift of ±5% may occur due to the ambient environment and exposure to laser radiation itself. The multilayer stack is porous and will absorb and desorb moisture. This results in a change in the refractive indices of the layers and produces a shift in performance characteristics. Through absorption of moisture high power UV coatings may become by composition 30% water.

Beam splitters and mirrors are designed to operate at a particular AOI. If they are used at other angles percentage transmission and reflection figures will shift away from their optimum and phase shifts will be introduced. This is undesirable in PTG systems since it will induce a

Departure from specification	Straight through Train (Train 1)		Detoured Train (Train 2)	
	% Beam Trans	%PHM	% Beam Trans	%PHM
-7%	39	35	40	48
-5%	39	48	40	56
-2%	39	77	39	72
Specification	39	84	39	81
+2%	39	68	39	77
+5%	40	42	39	60
+7%	40	30	39	51

Table(2): Performance estimates for System A. Figures for % beam transmission and %PHM (ratio of smallest pulse intensity to largest) are given. Trains (1) and (2) are obtained simultaneously and are complementary.

Departure from specification	Straight through Train (Train 1)		Detoured Train (Train 2)	
	% Beam Trans	%PHM	% Beam Trans	%PHM
-7%	38	31	36	70
-5%	38	31	36	71
-2%	38	32	36	69
Specification	38	33	36	67
+2%	38	35	36	65
+5%	38	38	37	63
+7%	39	41	37	63

Table(3): Performance estimates for System B. Figures for % beam transmission and %PHM (ratio of smallest pulse intensity to largest) are given. Trains (1) and (2) are obtained simultaneously and are complementary.

Departure from specification	Train 1 Single waveplate in position 1 only		Train 2 Single waveplate in position 2 only	
	% Beam Trans	%PHM	% Beam Trans	%PHM
-7%	52	37	53	51
-5%	52	50	53	60
-2%	52	77	53	73
Specification	52	86	53	81
+2%	52	70	53	76
+5%	53	45	53	58
+7%	53	33	53	48

Table(4): Performance estimates for System C. Figures for % beam transmission and %PHM (ratio of smallest pulse intensity to largest) are given. Note that trains (1) and (2) are not obtained simultaneously. Train (1) is obtained with a single waveplate in position(1), cf figure 7, only and Train(2) as given above is not its complement. Train(2) is obtained with a single waveplate in position(2) only.

shift away from a nominally desired splitting ratio.

Most dielectric surfaces become charged when irradiated with ultraviolet light which will also ionize oxygen and water vapour. The resulting ions form clusters with dust, oil and other air pollutants commonly found in the filters of air conditioning units. These clusters will be attracted to the charged dielectric surface forming a contaminant coating and causing the performance of the optic to deteriorate. Since it is not possible to protect a UV optic by coating it with a transparent conducting overcoat, as these become absorbing below 600nm, all such optics are should be protected in a flow box. [6]

Unless fluorescence is induced substrate losses may be taken to be negligible.

Birefringence in the substrate will disturb the polarization state of the pulse away from its linearly required state.

Wavefront distortion represents a change in the direction of propagation of the light pulse i.e. a change in the orientation of the electric vector with the plane of incidence of the optic. Therefore with respect to the wavefront it is a local depolarizing effect in that it represents a local angle of incidence error.

4 System Alignment

Accurate alignment is required in order simultaneously to

1. ensure the accuracy of the timing between the pulses of the train.

2. ensure that the pulses within the train travel the same path to the photocathode and are coincident on it.

3. obtain optimized optical performance at any mirror or splitter.

The principles according to which the generator optics may be geometrically aligned and the timing between the pulses set will be described in this section. Details of an integrated alignment procedure are presented in reference [8] where notes on how to specify optics, both those to be aligned and those to be used in the alignment beam, are to be found

4.1 Geometrical Alignment

The optics within the generator, cf figure 7, are required to be either parallel to each other e.g. M1 with S1, M2 with S2 and with M3 etc, or perpendicular to each other e.g. M1 with respect to M2, in order to provide a 180° detour. After having aligned the optics within the generator the synchro-laser pulses must inject into the system at an angle of 45°

Any two reflecting surfaces may be aligned parallel to each other using the technique developed by Bergman and Thompson [9]. This technique, cf figure 8 (not to scale), is based on the observation of Tolansky fringes [10],[11]. These non-localized circular fringes are formed when plane parallel reflecting surfaces are illuminated by a point source provided by focusing a collimated cw laser beam down through a pinhole in a screen. The diverging light from the pinhole is allowed to illuminate the surfaces to be aligned, M1 and S1 for example. When these surfaces are adjusted such that the back reflected light from each is superimposed on the pinhole screen Tolansky fringes will be observed. Assuming the optic furthest from the point source to be perpen-

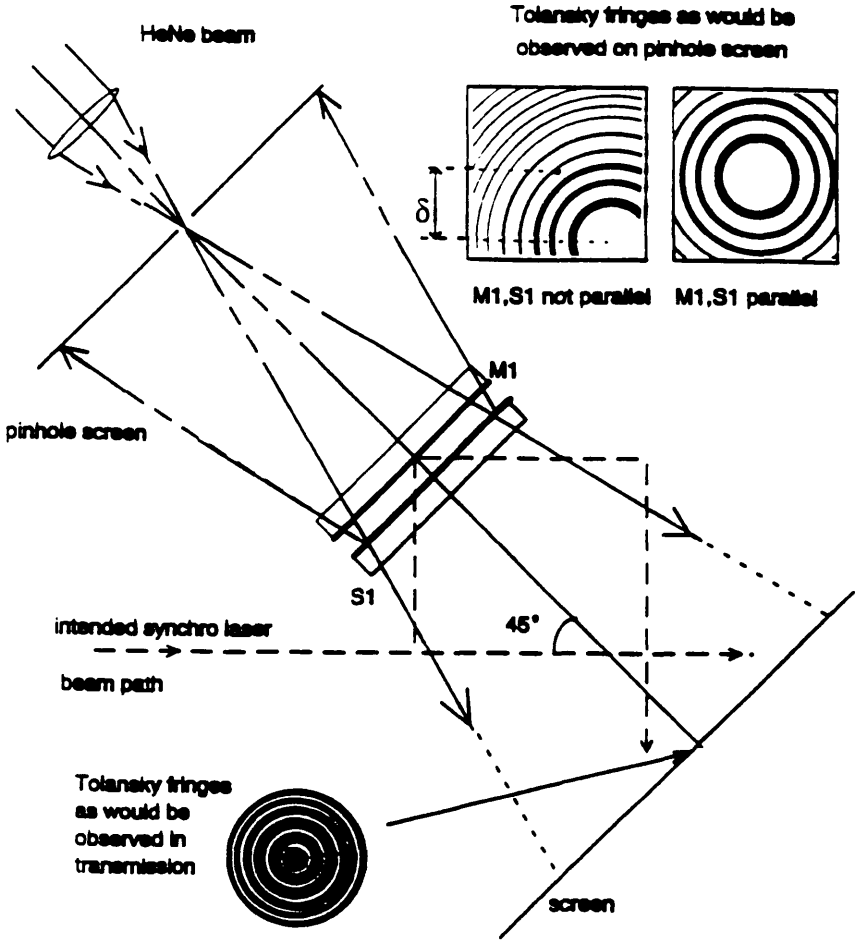

Figure 8: Observation of Tolansky fringes produced by two plane parallel reflecting surfaces, in this case the splitter coating of S1 and the reflective coating of M1, on illumination by a point source. When surfaces are parallel and perpendicular to the axis of the alignment beam the fringe system observed in reflection will be centred on the pinhole of the pinhole screen. A complementary system is also observed in transmission. (Diagram not to scale)

dicular to the axis of the alignment beam Bergman and Thompson show, that for $d \gg s$ where d is the distance between the pinhole screen and the optic furthest from it, i.e. S1, and s is the distance between the optics that α the angle between the surfaces is given by

$$\alpha = \frac{\delta s}{2d^2} \qquad (1)$$

where α is in radians and δ is the displacement of the centre of the fringe system from the centre of the pinhole as shown. When the reflecting surfaces are parallel to each other and perpendicular to the axis of the alignment beam the circular fringe pattern will be centred on the pinhole. Ford and Shaw [12] show, for the complementary fringe pattern in the transmitted light, that

$$\alpha = \frac{\delta s}{(d+l)d} \qquad (2)$$

where l is the distance between the optic furthest from the point source and the screen placed after it. In this case the residual tilt is indicated when the secondary maxima cross the primary maxima [13]. Having aligned M1 parallel to S1, S1 may be displaced to its required

position.

The principles used to align two optics parallel to each other, and perpendicular to the axis of the alignment beam, may be used to align them perpendicular to each other in order to provide the 180° detours. A total internal reflection prism (TIR), cf figure 9, is placed in the space between the two mirrors such that it is the axis of the alignment beam which is bent through 90°. Aligning the mirrors perpendicular to the beam axis is equivalent to aligning them parallel to each other and Tolansky fringes will be observed.

To apply the techniques described here the optics of the generator are mounted on carriages which slide along rails as shown in figure 10. In practise all optics are aligned with a TIR in the alignment beam and use is made of a reference mirror (RM).

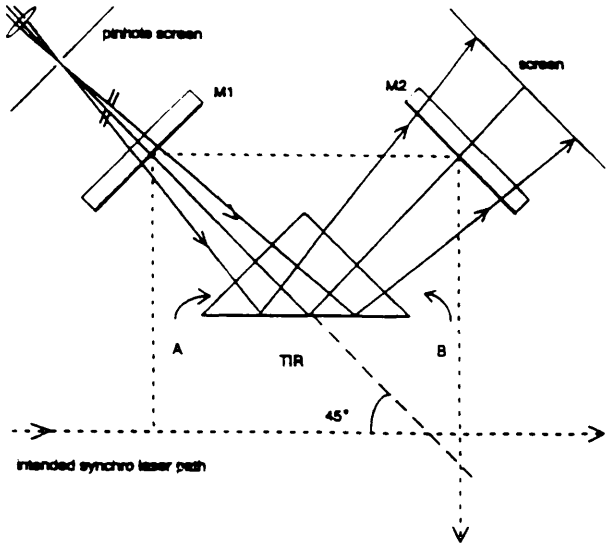

Figure 9: Configuration using a total internal reflection prism (TIR) allowing the observation of Tolansky fringes, between two plane parallel reflecting surfaces of mirrors M1 and M2 required to provide a 180° detour. Fringes will be observed in reflection on a pinhole screen and in transmission as illustrated in figure 8. For purposes of clarity reflected beam paths are not shown. (Diagram not to scale)

4.2 Timing

Having completed the geometrical alignment the timing between the pulses within the train may be set. Recent calculations based on the vectorial additional of the 30 GHz field contributions from the individual electron bunches, generated by the train of laser pulses, indicate that both the cumulative timing error between the first and last pulses and the relative error between any two consecutive pulses should be less than 2 ps. Three stages are required to generate an eight pulse train. If the stage error is taken to be e then the maximum cumulative error that can occur is $\pm 3e$. The maximum relative error is also of magnitude $3e$ and is generated in the case where errors of $-e, +e$ and $+e$ occur in stages 1, 2 and 3 respectively. Thus $3e \leq 2$ ps. In practise it is not the

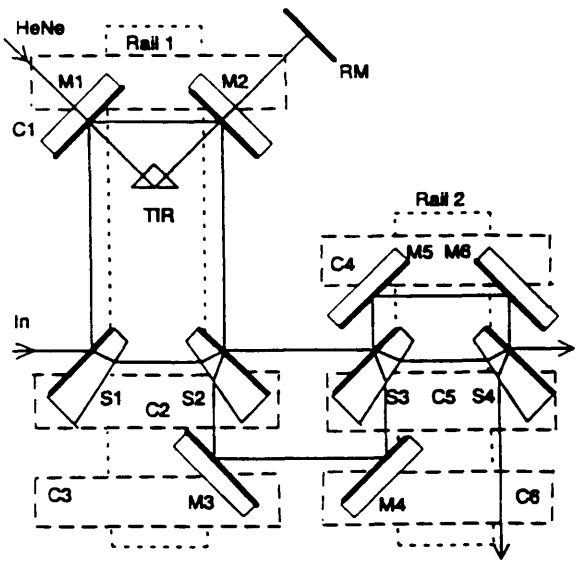

Figure 10: Schematic diagram indicating how the beam splitters, S1 to S4, and mirrors, M1 to M6, are mounted on carriages C1 to C6 and rails. Heavy lines denote the actual mirror and beam splitter coatings. RM and TIR are optics required for the HeNe alignment beam.

entire stage paths that are measured but the detour lengths l_1, l_2, and l_3, cf figure 1. Thus $e_l \leq 1/3$ ps where e_l is the error in the detour length l.

Figure 11. illustrates how the timing in stage 1 may be set. The procedure consists of bringing reflecting surfaces, which have already been aligned parallel to each other, close together until the distance between them may be taken to be zero. One surface is then be displaced a known distance with respect to the other.

Rather than using visual inspection, Tolansky fringes viewed in transmission, may be used to determine accurately when the distance between two reflecting parallel surfaces is small enough to be taken as zero. As the distance between the surfaces is reduced the diameter of the fringes, will be observed to grow. The angular diameter ϕ_p of the p^{th} fringe is given by

$$\phi_p = \sqrt{\frac{4p}{t}} \qquad (3)$$

where t is the distance between the surfaces [14]. In an optimized alignment beam it should be possible to set the separation of the surfaces accurately without allowing them to touch. If the aligment beam is not sufficiently optimized an estimation of the surface separation may be obtained by observing the relative displacement of the Tolansky fringes when the optics are allowed to lightly push against each other. In this case an abrupt displacement of the centre of the fringe system will be observed when one optic begins to push against the other. Using an interferometer this method was measured to give a t=0 distance accurate to 0.07 ps. In practise the alignment beam used for geometrical aligment will not be suitable for setting the t=0 distances [8]. Instead a compact monitor, t=0 monitor, consisting of a laser and lens combination which will provide

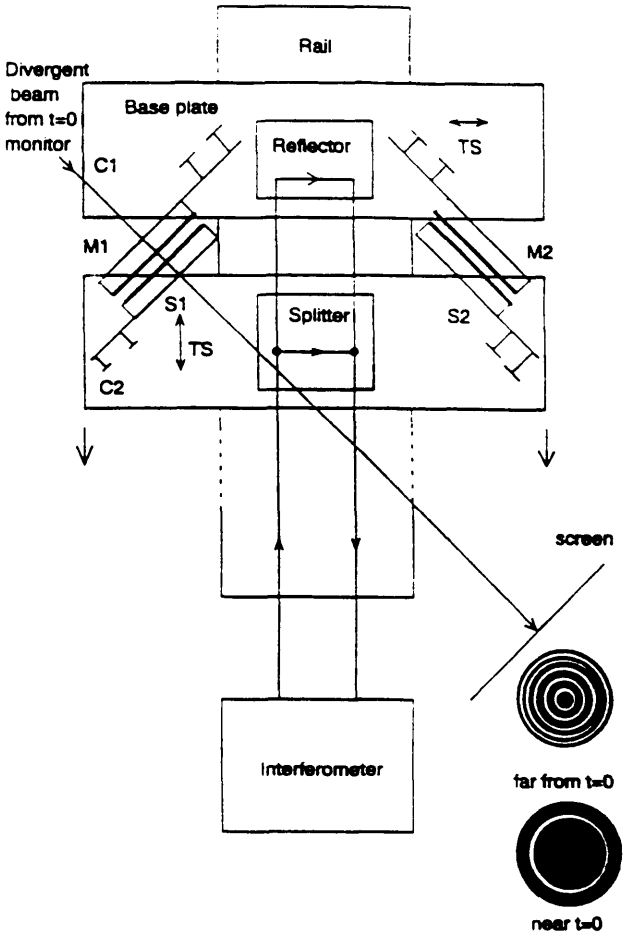

Figure 11: Illustration of how the timing in stage 1 may be set. Mirrors M1 and M2 and splitters S1 and S2 are mounted on carriages C1 and C2 such that M1 and S1 (and similarily M2 and S2) may be brought close together, using the translational stages TS, so that the t=0 distance may be set. The divergent beam from the t=0 monitor generates the Tolansky fringes as shown on a distant screen. The interferometer reflector and splitter optics are mounted in the middle of the carriages as shown with the interferometer aligned parallel to the rail.

a highly divergent beam is required.

To determine the 't=0' distances between M1, S1 and M2, S2 carriage C2, cf figure 11, is slid close to C1 so that the optics are a few mm apart. Then with the t=0 monitor S1, which is mounted on a translational stage (TS), may be moved towards M1 until the distance between them is deemed to be zero. The t=0 monitor may then be moved behind M2 and the t=0 distance between M2 and S2 set by adjusting the TS on which M2 is mounted. Having determined both t=0 settings carriage C2 may be displaced with respect to C1 to give the detour length required. This displacement is measured interferometrically, the optics of the interferometer having been mounted on the carriages and the interferometer aligned along the axis of the rail before the t=0 settings were made. To facilitate fine tuning of the separation, translational stages are mounted between the base plate of the carriage and that part of the carriage which slides along the rail.

Using the technique described above, the detour lengths of the stages are set between reflecting surfaces (indicated by the thick black lines on the optics in figure 10.) When calculating the actual physical lengths of each of the detours, allowances must be made for the fact that some pulses within a stage travel only in air whilst others are slowed down by travelling through substrate material and are beam walked by it. Account must also be taken of the fact that the radio frequency is only nonimally 3 GHz, being in practise 2.9986 GHz and that therefore the pulse separation required is 333.49 ps.

It is possible to use the procedures described here to obtain a direct measure of detour length because the geometry of the PTG allows the reflecting coatings to be brought close together, so the t=0 distance may be set, and then for one to be displaced to achieve the required detour length. In a system built to operate at the Brewster angle it would not be possible to set the t=0 in the manner described and therefore indirect methods of setting the timings between the pulses to a high accuracy would be required.

4.3 Factors limiting alignment and timing

The accuracy of the geometrical alignment is determined by the accuracy to which the mirrors and splitters may be aligned parallel to each other. Accuracies better than 2 seconds of arc are possible. In stability tests, of duration three days, this degree of parallelism was maintained.

The degree to which it is possible to make all the pulses colinear along the beam path between the output of the generator and the photocathode is a function of the wedge angle of the beam splitter substrates [8]. For example if substrates with a wedge angle of a few seconds of arc are used then the pulses produced by the train will hit the photocathode 20m away to within a few mms.

The accuracy of the method used to set the timing between the pulses is limited by

1. the accuracy of the interferometer; estimated to be about 0.003 ps
2. the determination of t=0 distance; estimated to be less than 0.07 ps
3. the sensitivity of the translational stages mounted below the base plates of the carriage. In principle accuracies of about 0.003 ps should be obtainable but sometimes this

was found to be of the order of 0.03 ps.

4. the accuracy of the stage alignment; for example if the stage alignment is accurate to 11 seconds of arc then the timing error induced will be of the order of 0.09 ps.

5. substrate wedge angle; this error will be induced by virtue of the fact that the pulses will not travel colinearly to the photocathode but will each take a path of slightly different length. When the substrate wedge angle is in the order of seconds of arc the difference in total path length will be negligible (errors in the order of femtoseconds).

6. tolerance on the substrate thickness; An error of 0.15 mm in thickness (typical tolerance quoted for a 9.5 mm thick substrate) will introduce a timing error of 0.32 ps at each substrate encountered. Substrate thicknesses must be measured.

If substrate thicknesses are measured, as they were in the present case, the overall accuracy to which the timing between the pulses may be set is better than the 0.33 ps required. To attain this accuracy the rails on which the generator is built must be aligned parallel to each other and the direction of motion of the various translational stages on the carriages used aligned with respect to the axis of these rails. Also carriages must locate accurately along the lengths of the rails.

The above method of setting 't=0' is such that it guarantees, for example, that the separation of the reflecting surfaces of S1/S2, cf figure 11, is equal to that between those of M1/M2. Therefore in a correctly aligned stage provided that the substrates of S1 and S2 are of equal thickness, and, that the input pulse is injected at an angle of 45° with respect to S1, then the detoured and straight through pulses of the stage will be observed to be exactly coincident at the output of the stage and the pulses will be observed to follow the same path in the next stage. In this case the stage alignment error will be seen as the separation of the pulses on a distant target. In the case where there is an injection error [8] the two pulses will not be coincident at the output of the stage. An injection error therefore presents itself as an apparent geometrical alignment error and induces a timing error since it means that pulses within the stage do not travel parallel and perpendicular to the axis of the rail, parallel to which the interferometer has measured the separation of the reflecting surfaces of the optics.

5 Experimental results

The layout of the optics used is presented in figure 12. The 15 ps (FWHM) pulses at the output of the synchro-laser were synchronised with respect to the RF field with a timing jitter, measured in the green (524 nm) to be less than 1 ps. Pulse energy was of the order of 60 to 80 μJ at 209 nm. Before being injected into the PTG these pulses were expanded using a Galilean telescope (a) to a diameter of approximately 10 mm. A Rochon prism (e) was required to ensure that the pulses entering the PTG would be S-polarized. To maximize throughput of the polarizer a $\lambda/2$ waveplate (d) was placed in front of it. This waveplate was tilted with respect to the axis of the synchro-pulse so that it acted as a poor compensator. The PTG system constructed was system C with waveplates (p) and (k) in the intended positions as shown in figure 12. A second Galilean telescope, not shown in figure 12, was used in reverse and positioned approximately half way along the 20 m beam path to the photocathode. Its pur-

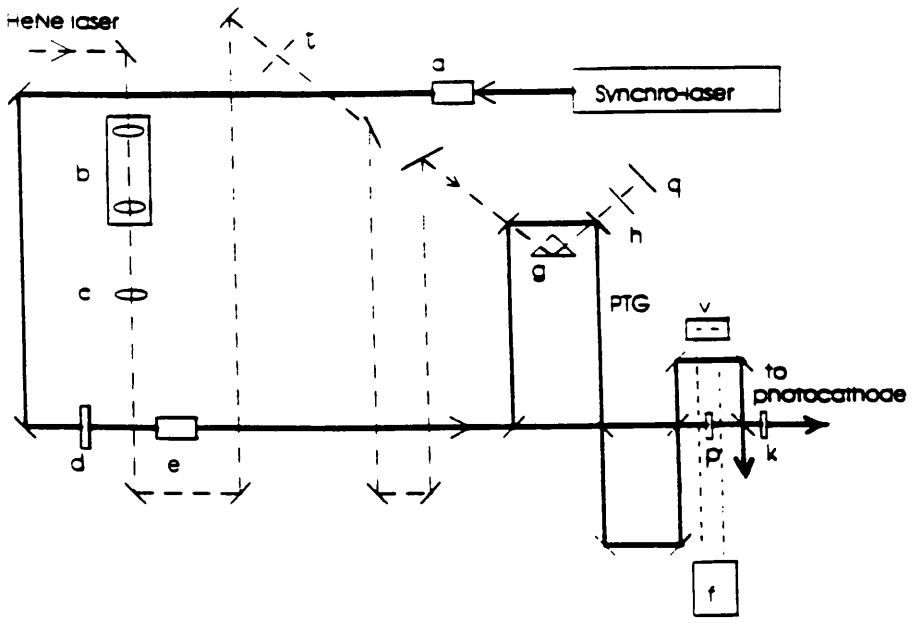

Figure 12: Layout of optics on granite table. Heavy line indicates the path of the synchro-laser pulse with Galilean telescope (a), $\lambda/2$ waveplates (d) and (p), Rochon prism (e), and $\lambda/4$ waveplate (k). Broken line indicates the HeNe alignment beam used for geometrical alignment with collimator (b), 2.5m focal length lens (c), pinhole screen (t), TIR prism (g), reference mirror (h) and screen (q). Dotted line shows interferometer (f) beam line along rail 2 of the PTG, reflector optic (v) only shown.

pose was to provide adequate pulse imaging onto the photocathode. A spot size of 6 mm diameter on the photocathode was intended but triangular images of 6mm by 9mm were observed. The dashed line in figure 14 indicates the beam path of the alignment laser used for the geometrical alignment of the system. The pinhole screen (t) is approximatley 2.5 m from the optics to be aligned. The dotted line indicates the interferometer beam line which would be used to set the timing on rail 2 of the generator. For the sake of clarity only the reflector optic is shown.

The %PHM (i.e. the ratio of the smallest to largest pulse intensity) obtained with system C, as shown in figure 12, was poor being in the order of 25%. By inserting additional waveplates into the stages it was possible to improve this to 45%. In this case the settings of the additional waveplates, which had been inserted into stage 1, had been fully optimized but the settings of those inserted into the other stages were not. A streak camera picture of the train of laser pulses taken at the output of the PTG is presented in figure 13.

Having generated the train the timing between the pulses was investigated, with the use of a streak camera, by measuring the time interval between pairs of consecutive pulses i.e. pulses 1 and 2, 2 and 3 etc. The camera was calibrated using electron pulses generated by LIL which are bunched at the RF frequency of 3 GHz. With the exception of pulses 4 and 5, it would appear that the timing between the pulses of the train, cf table 5, is good to within the 4 ps resolution of the streak camera. However a very large timing error of the order 16 ps is clearly evident between pulses 4 and 5.

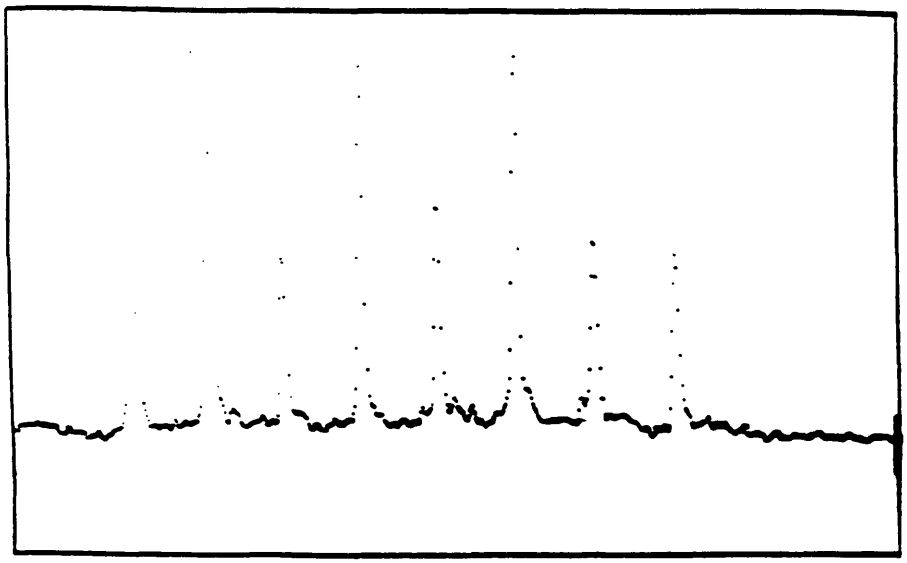

Figure 13: Streak camera picture of train of laser pulses taken at output of the PTG. Full image width corresponds to 3.59 ns.

The synchro-laser may be operated to output two pulses with a separation of 4 ns at a frequency of 10 Hz. Using two such pulses to generate two trains of eight, 10 MW of RF peak power at 30 GHz was generated using the CLIC transfer structure. This was achieved using trains which had a %PHM of better than 25% and with the timing error of 16 ps, in the first stage as measured using the streak camera, corrected by suitable adjustment of the translational stage of the carriage supporting mirrors M1 and M2. Laser energy per train at the photocathode was of the order of 4 μJ.

Pulses recorded	Pulse separation/ps
1,2	334
2,3	331
3,4	337
4,5	317
5,6	335
6,7	331
7,8	334

Table 5: Separation of pulse pairs within the train as measured using a streak camera (resolution of 4ps)

6 Conclusions and discussion

Given that the beam input into the PTG was correctly polarized the ability to increase the %PHM within the generator by the insertion of waveplates indicates that depolarizing effects are being introduced within the generator. The improvement of the %PHM is possible in this case because use is made of the separation of the S- and P-polarization curves of the 50:50 S-polarization splitters. In fact what has been constructed is an unoptimized compensated system. On testing the splitters from the coating side (as opposed to the substrate side) a splitting ratio of 50:50 was obtained as expected. On analysing the performance of stage 1 it was found that the detoured pulse on interaction with S2 from the coating side was split 53:47 indicating that any depolarizing influences within the stage detour are minimal. However the pulse transmitted through S1 was not equally split on interacting with the

splitter coating of S2 from the substrate side, a splitting ratio of 30:70 being observed. This would indicate that the substrate may be shifting the polarization state of the pulse away from its required S-polarization state. A problem of birefringence is therefore suspected and this must be investigated. Should such a depolarizing effect prove to be unavoidable simple systems should be abandoned for this wavelength and compensated systems considered.

To insure the coincidence of the pulses on the photocathode 20 m away very parallel substrates (wedge angle less than 2 seconds of arc) were used. Their thickness (9.24 mm) however was sufficent to prevent the 15 ps pulses from producing interference effects within the substrate. If this had been the case a 50:50 splitting ratio would not at any time have been obtained.

With respect to timing a very large error of approximately 16 ps was produced between pulses 4 and 5 indicating an error of 16 ps in the first stage of the generator. Incorrect injection of the pulse from the synchro-laser into the PTG itself is one source of timing error which has not been adequately investigated. Insufficient care was taken to guard against this error and when it was observed it was misinterpreted and the system inappropriately adjusted. Instead of correcting the injection error the distances between the detour mirrors of stages 1 and 2 were adjusted to make the pulses coincident at the stage outputs. In this manner the system was corrected to allow for an apparent geometrical alignment error and a train of eight pulses colinearly aligned and coincident to within 1.5 mm on the photocathode, 20 m away, was obtained. The injection error however remains uncorrected in this instance.

Acknowledgements

The author would like to thank Professor J. Ebert of Laseroptik for his many useful discussions and permission to reproduce figures and data supplied by Laseroptik. The author is also grateful to S. Hutchins, for technical support and for preparing the diagrams for this publication, K.K. Geissler, S. Schreiber and I.Kamber (synchro-laser), E.Keller (alignment of rails and translational stages), S. Battisti and J.C. Thomi (streak camera),the CERN workshops and the staff of the Photocathode and Lasers Section, LP group, and the team running the CTF for their support and encouragement.

Appendix: List of abbreviations

AOI, angle of incidence
CAS, CLIC accelerating structure
CLIC, CERN linear collider
CTF, CLIC test facility
FWHM, full width half maximum
LEP, large electron positron collider
LIL, LEP injection linac
PTG, pulse train generator
PHM, pulse height modulation (ratio of the smallest pulse intensity to largest)
RF, radio frequency
RM, reference mirror
TIR, total internal reflection prism
TS, translational stage
UV, ultra-violet

References

1. K. Hübner, *Generation of 30GHz RF power in the CLIC Test Facility,* CERN PS 91-06(LP).

2. J.P. Delahaye, *A simplified scheme for 30GHz generation in the CTF,* CERN PS 92-44(LP).

3. M. Yoshioka, *Lasertron, A Pulsed*

RF-source using Laser Triggered Photocathode, INS-Rep.-726. Dec 1988. University of Tokyo.

4. K.K. Geissler, *Generation of Short Laser Pulses,* this workshop.

5. J.P. Delahaye, J.H.B. Madsen, A. Riche, L. Rinolfi, *Present status and future of the CERN Linear Collider Test Facility (CTF),* this workshop.

6. J. Ebert, Laseroptik, Garbsen, Germany, *Private communication.*

7. R.W. Ditchburn, *Light,* Academic Press, London, New York, San Francisco, 1976.

8. P.M. Devlin-Hill, *Geometrical alignment and timing of 45° Pulse Train Generators,* CERN PS 93-40(LP).

9. T.G. Bergman, J.L. Thompson, *An Interference Method for Determining the Degree of Parallelism of (Laser) Surfaces,* Appl. Opt., **7**, 923 (1968).

10. S. Tolansky, *New Non-Localized Interference Fringes,* Philos. Mag., **34**, 555 (1943)

11. N. Aebischer, *Calculs de Profils Dissymétriques Observables sur des Figures d'Interférences en Ondes Multiples Sphériques,* Nouv. Rev. Opte. Appl., **2**, 351 (1971).

12. D.L. Ford, J.H. Shaw, *Rapid Method of Aligning Fabry-Perot Etalons,* Appl. Opt., **8**, 2555 (1969).

13. D. Malacara, *Optical Shop Testing,* John Wiley and Sons, New York, 1978.

14. S. Tolansky, *Multiple-Beam Interferometry of Surfaces and Films,* Dover, New York, 1970.